Modelling the Effects of Friction on Tool-Chip Interface Temperature During Orthogonal Cutting of Al6061-T6 Aluminium Alloy

Sunday Joshua Ojolo, Sikiru Oluwarotimi Ismail and Kelechi Ogbuanu
Department of Mechanical Engineering
University of Lagos
Akoka-Yaba, Lagos, Nigeria
sojolo@unilag.edu.ng, sismail@unilag.edu.ng

Abstract

In this work, finite element simulations based on the analytical model derived with the MATLAB software were used to establish the temperature fields within the cutting tool and tool-chip interface. The average tool-chip interface temperature model was simulated and the simulation results were compared with experimental results for validation. At a maximum cutting speed of 90 m/min, the maximum temperature obtained from the experiment was 410 ^{o}C, at same rake angle of 0^{o}. However, the developed model predicted 490 ^{o}C under the same conditions. The higher value obtained by the model can be attributed to the negligence of heat losses to the surrounding by both convection and radiation modes, as an assumption in the formulated model. A similar trend of these results was also recorded for the case of rake angle and feed rate of 30^{o} and 0.0635 mm/rev, respectively. It was observed that the simulation results and experimental measurements for the average tool-chip interface temperature agreed significantly.

Keywords
Machining parameters, tool-chip temperature, friction, finite element, simulation results.

1. Introduction

The process of machining has been a subject of research over the last six decades (Kegg, 1965; Astakhov, 1999; Altintas, 2000). Friction plays an important role during cutting of materials, as the cutting tool and workpiece continuously rub or slide on each to transform the material from elastic stage to plastic phase, where permanent shear or cutting takes place. Therefore, it is imperative to understanding the machining parameters that affect frictional force. Also, cutting parameters must be optimised to minimise the friction since average of 55% of the energy consumed during machining process is used to deform materials and causes chip formation. If it is non-optimised process, greater part of the remaining energy is used for the conversion of the useful energy to the heat energy, from interface temperature between tool-workpiece and chips (Astakhov, 2006). Consequently, a stable cutting machine, less time, cutting and energy consumption/power are possible with when a cutting forced is reduced (Astakhov, 2005). The importance of the machining parameters cannot be undermined toward determination of the efficiency and effectiveness of a machining operation. The process of machining is affected by several parameters. These include, but are not limited to, depth of cut, tool rake angle, cutting speed, cutting tool edge angle, feed rate and the properties of the workpiece materials used (Bayoumi et al., 1994).

As the advent of machining technology increases, many researchers have been attempting to establish a relationship between these parameters and process mechanics. They included sophisticated mathematical formulations of frictional behaviour on the cutting tool rake face, high temperature, high strain rate and work-hardening of the workpiece material. In addition, many techniques based on finite element methods have been adopted to establish several models and optimise the whole concept of machining technology. These methods include, but are not limited to, element separation, mesh rezoning, modeling worn cutting tool geometry and friction modeling. They were all used to predict the orthogonal metal cutting (Strenkowski et al., 1985; Strenkowski et al., 1987; Komvopoulos et al., 1991; Ueda et al., 1992; Shih et al., 1993; Shih et al., 1995;). For example, Shih et al. (1993) developed and implemented a finite element model for the simulation of plane strain continuous chip formation during orthogonal metal cutting process. Categorically, some of these studies were concentrated on tool wear (Hartung and Kramer, 1982; Gerez et al., 2009; Ezugwu and Wang, 1997; Yen et al., 2004; Dogra et al., 2011), cutting force (Babu et al., 2008; Kim and Ehmann, 1993; Ozel and Altan, 2000) chip formation (Salem et al., 2012; Abushawasi et al., 2011) and cutting temperature or heat generation/transfer (Mottaghizadeh and Bagheri, 2012; Pittalà and Monno, 2011; Jam and Fard, 2011; Alabi et al., 2012; Kagnaya et al., 2011; Zhang et al., 2015) during machining processes.

However, it must be noted that most of the extant works have been concentrated on several cutting parameters and conditions, with a very scarce and limited studies on effect of friction during orthogonal machining, especially on Al6061-T6 aluminum alloy material using combined approach. Hence, in this work, a combination of analytical and finite element methods (FEM) are adopted to examine the effects of several variables (related to tool-chip interface friction) on the average and maximum interface temperature between cutting tool and chip in orthogonal machining using a single point cutting tool.

2. Models Development

2.1 Friction force model

Experiments conducted by several researchers have shown that the normal pressure acting at the tool-chip interface varies exponentially, such that it is maximum at the tool tip and diminishes to zero at the point where the chip separates from the rake face of the tool (Moufki et al., 1998; Tao et al., 2004; Childs, 2006), as illustrated in Figure 1. The normal stress is distributed along the rake face of the cutting tool.

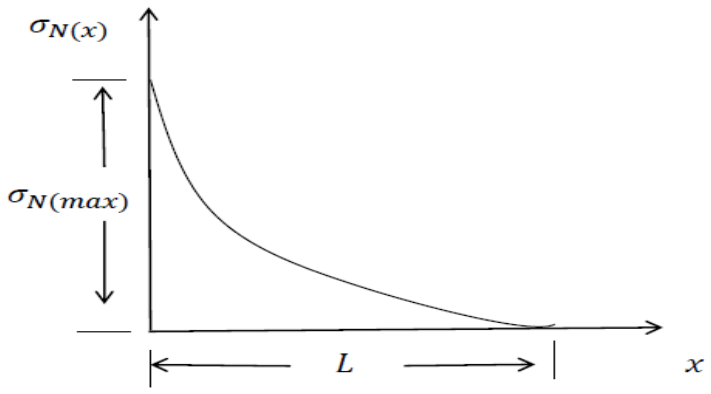

Figure 1 Illustration of normal stress acting at tool-chip interface.

Therefore, the mathematical equation of the curve in above Figure 1 is as follows:

$$\sigma_{N(x)} = \sigma_{N(max)} \left[1 - \left(\frac{x}{L}\right)^n \right] \quad (1)$$

Where $\sigma_{N(x)}$ represents the exponential pressure distribution, $\sigma_{N(max)}$ represents the maximum pressure acting along the rake face of the cutting tool, x is the distance measured from the cutting tool tip along the cutting tool rake face, L is the contact length of the interface between tool and chip and n represents the control parameter for pressure distribution.

The frictional resistance acting at the interface between tool and chip is not continuous along the cutting tool's rake face. It consists of two components (Figure 2). These are:

(i) Static component of friction

(ii) Dynamic component of friction

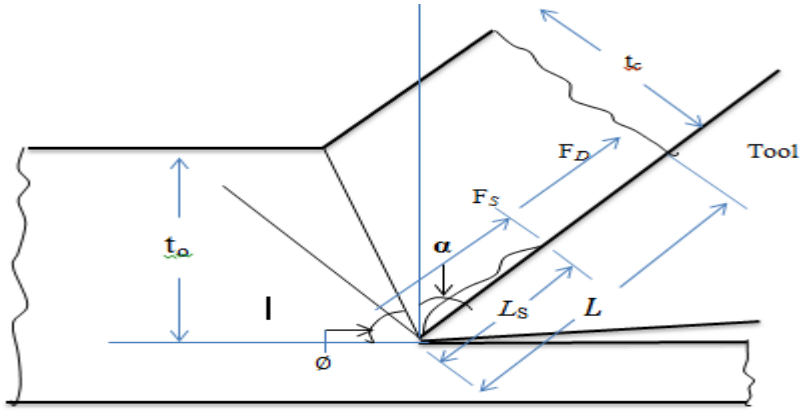

Figure 2 Friction force comprising of static and dynamic components in orthogonal cutting.

The static component (F_{ST}) is due to the developed built-up edges which stick to the region around the cutting tool tip. This built-up edge induces a constant shear stress (τ) within the sticking length (L_S). The total frictional resistance (F_T) can then be expressed mathematically as:

$$F_T = F_{ST} + F_D \quad (2)$$

Since F_{ST} is known to be constant along the sticking region, the static frictional force can be written as:

$$F_{ST} = \int_0^{Ls} w.\tau.dx = \int_0^{Ls} w.k.dx \quad (3)$$

$$F_{ST} = w.L_S.k \quad (4)$$

Where w represents the width of cut and τ is supposed to have the same value with the shear flow stress, k of the workpiece material. The dynamic component (F_D) depends on the sliding motion of chip along the rake face of the cutting tool.

$$F_D = \int_{Ls}^{L} w.\mu.\sigma_{N(x)}.dx \quad (5)$$

By substituting Equation (1) into Equation (50, Equation (5) becomes:

$$F_D = \int_{Ls}^{L} w.\mu.\sigma_{N(max)}.\left[\ 1 - \left(\frac{x}{L}\right)^n \right].dx \quad (6)$$

$$F_D = w.\mu_a.\sigma_{N(max)} \left\{\frac{\left[nL - Ls\left[(n+1)-\left(\frac{Ls}{L}\right)^n\right]\right]}{n+1}\right\} \quad (7)$$

The total frictional force acting at the interface between tool and chip is therefore established after both Equations (7) and (4) are substituted into Equation (2). Thus, it becomes Equation (8):

$$F_T = w.\mu_a.\sigma_{N(max)}.\left\{\frac{\left[nL - L_s\left[(n+1)-\left(\frac{L_s}{L}\right)^n\right]\right]}{n+1}\right\} + w.L_s.k \quad (8)$$

2.1.1 Maximum normal pressure acted at tip of the cutting tool, $\sigma_{N(max)}$

The highest normal pressure occurred at the cutting tool tip is calculated by applying slip-line field indentation theory. This theory is established on a plastic deformation of materials. It is geometrically self-constant and is stationary permissible. The planes of highest shear stress are slip lines. They exhibit 45° orientation to the principal stresses. This theory has some assumptions such as homogeneity and isotropy of the workpiece material, zero strain hardening, prevalence of deformation from plain strain, negligible effects of strain rate and temperature, among others.

The normal pressure at the tool tip is given as:

$$\sigma_{N(max)} = 2k\,(ø - \alpha) + k \quad (9)$$

Where Ø, expressed in terms of α, is

$$Ø = \tan^{-1}\left[\frac{r\cos\alpha}{1 - r\sin\alpha}\right] \quad (10)$$

Where, ø represents shear angle, α is the rake angle and r is the chip thickness ratio.

2.1.2 Contact length of the interface, L between tool and chip

The contact length of the interface between tool and chip can be determined from triangle *AOE* in Figure 3

$$L = t_o\ \left[\frac{\sin[\frac{\pi}{4}+Ø-\alpha]}{\sin Ø \sin\frac{\pi}{4}}\right] \quad (11)$$

2.1.3 Sticking length of the interface, L_S between tool and chip

The sticking size of the built-up edge is approximately equal to the length or line *AD* on triangle *AOD* (Figure 3).

$$L_S = t_o \frac{\sin(\emptyset - \alpha)}{\sin \emptyset} \quad (12)$$

2.1.4 Sliding frictional force at interface, F_D between tool and chip

Considering Equation (7), the total frictional force F_D becomes:

$$F_D = \frac{w\, t_o \tan[\alpha + \tan^{-1}(Fc / Ft)]\,[2k(\emptyset - \alpha) + k]}{n+1} \left\{ n \left[\frac{\sin[\frac{\pi}{4} + \emptyset - \alpha]}{\sin \emptyset \sin \frac{\pi}{4}} \right] \left[\frac{\sin(\emptyset - \alpha)}{\sin \emptyset} \left[(n+1) - \left(\frac{\sin(\emptyset - \alpha) \sin \frac{\pi}{4}}{\sin[\frac{\pi}{4} + \emptyset - \alpha]} \right)^n \right] \right] \right\} \quad (13)$$

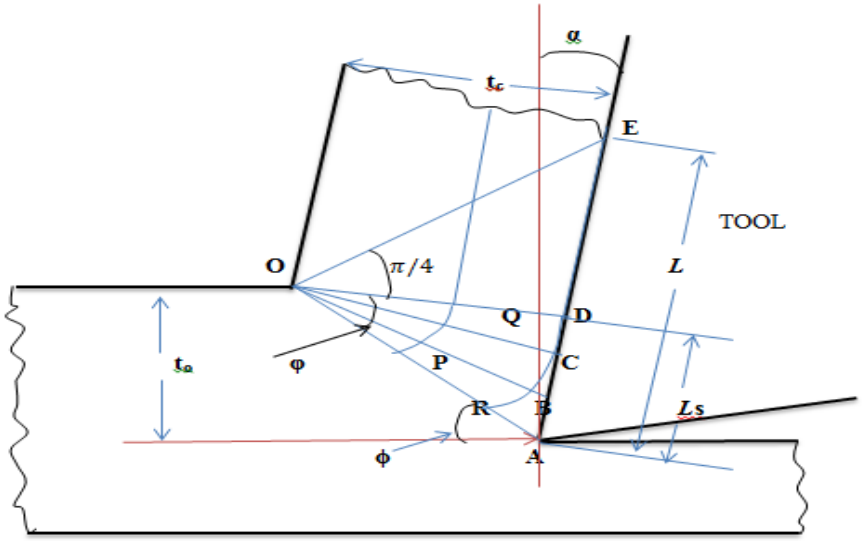

Figure 3 Schematic for slip-line field in orthogonal cutting.

2.2 Frictional heat and temperature modelling

Production of heat energy during orthogonal machining is primarily due to plastic deformation, occurs at the primary shear plane (shear zone) and friction at the interface between tool and chip. The tool-chip interfacial friction and plastic deformation at primary shear region affect the average interfacial temperature generated between the tool and chip.

2.2.1 Average interfacial temperature, T_{int} between tool and chip

During orthogonal cutting processes, the rate at which mechanical energy (as a results of the dynamic friction developed at the interface between chip and tool) is converted to heat, Q. This can be expressed mathematically as:

$$F_D\ V_C = Q \quad (14)$$

The quantity of the frictional heat energy rate (Q) assigned to the chip is determined by the coefficient of heat barrier (μ) such that, $0 \leq \theta \leq 1$ occurs at the interface between tool and chip. Hence,

$$F_D\ V_C(1 - \theta) = \dot{m}\, C_p \Delta T = (1 - \theta)Q \quad (15)$$

$$\dot{m} = \rho\, t_o\, w V \quad (16)$$

Therefore,
$$\Delta T = \frac{F_D\,(1-\theta)\,\sin\emptyset}{\rho\, C_p\, t_o\, w\, \cos(\emptyset-\alpha)} \quad (17)$$

F_D is the average dynamic friction force at the interface between tool and chip, V_C is the velocity experienced by the chip usually along the rake face, V denotes cutting speed, ρ represents the density of the workpiece, $\dot{m}$ represents chip mass flow rate of the chip, C_p represents the specific heat capacity of the material (workpiece) and $\mathbf{t_o}$ denotes the depth of cut.

The average interfacial temperature, T_{int}, between tool and chip can be estimated as the sum of the average shear plane temperature T_s and the average interfacial temperature rise between the tool and chip is represented by ΔT.

$$T_{int} = T_s + \Delta T \quad (18)$$

Where the average temperature at shear plane T_s can be determined by equating the heat energy absorbed by the chip along the shear plane with the shearing work along the shear plane as follows:

$$(1-\beta)\; F_S\; V_S = \dot{m}\, C_p\, (T_1 - T_o)$$

Hence,

$$\mathbf{T_s} = \mathbf{T_o} + \frac{(\mathbf{1-\beta})\; \boldsymbol{F_s}\; \mathbf{cos}\alpha}{\boldsymbol{\rho\, C_p\, t_0\, w}\; \mathbf{cos}(\emptyset-\alpha)} \quad (19)$$

$$\mathbf{T_{int}} = \mathbf{T_o} + \frac{(\mathbf{1-\beta})\, \boldsymbol{F_s}\; \mathbf{cos}\alpha + (1-\theta)\, \boldsymbol{F_D}\, \mathbf{sin}\,\emptyset}{\boldsymbol{\rho\, C_p\, t_0\, w}\; \mathbf{cos}(\emptyset-\alpha)} \quad (20)$$

Where β represents the amount of the energy produced in the primary region, absorbed by the Al6061-T6 aluminum alloy/workpiece (Oxley, 1989).

And

$\beta = 0.5 - 0.35\log(R_T \tan\emptyset)$ for $0.04 \leq R_T \tan\emptyset \leq 10.0$

$\beta = 0.3 - 0.15\log(R_T \tan\emptyset)$ for $R_T \tan\emptyset > 10.0$ (Oxley, 1989)

Where R_T is generally represented as: $\boldsymbol{R_T} = \frac{\boldsymbol{\rho C_P V t_o}}{\boldsymbol{K_t}}$

From Equations (20) and (21), $\mathbf{T_o}$ is the initial workpiece temperature which is supposed to be equal to room temperature in this study, F_S denotes the shear force acting along the shear plane, w denotes the chip width and ΔT represents average interfacial temperature rise in between the tool and chip.

2.2.2 Steady-state tool temperature distribution

Based on the conservation of energy, a very small fraction of the differential control volume of the cutting tool is expressed on the condition that the tool has orthogonal cutting geometry. Assuming two-dimensional steady heat conduction, without internal heat generation. The quantities Q_X and Q_Y representing the conduction heat rates are at right angle to both control surfaces, at coordinate locations of x and y, respectively. Using the Taylor

series expansion to express these rates at opposite surfaces, while terms of higher order are neglected to produce Equations (21) and (22), as thus:

$$Q_{x+dx} = Q_x + \frac{\partial}{\partial X}(Q_x)\,dx \tag{21}$$

$$Q_{y+dy} = Q_y + \frac{\partial}{\partial Y}(Q_y)\,dy \tag{22}$$

From the principle of conservation of energy,

$$Q_{in} - Q_{out} + Q_g = 0 \tag{23}$$

Therefore, knowing that the conduction rates establish the energy inflow, Q_{in}; energy outflow, Q_{out}; and energy generated, $Q_g = 0$, substituting Equations (21) and (22) into (23), we obtain

$$Q_x + Q_y - Q_{x+dx} - Q_{y+dy} = 0 \tag{24}$$

$$\frac{\partial^2 T}{\partial x^2} + \frac{\partial^2 T}{\partial y^2} = 0 \tag{25}$$

Which simplifies to:

Equation (25) is a two-dimensional elliptic partial differential equation (PDE). This Equation can be solved numerically by FEM with the MATLAB software, subject to the following boundary conditions at the interface between tool and chip, as depicted in Figure 4:

$$Q_{(0,Y)} = \begin{cases} \dfrac{F_D\, V_C\, (1-\theta)}{A_L} & \text{For } L_S \le y \le L \\ \dfrac{F_S\, V_C\, (1-\theta)}{A_S} & \text{For } 0 \le y \le L_S \end{cases} \tag{26}$$

Where A_S and A_L represent the cross-sectional areas of the sticking and sliding regions at the the interface between tool and chip, and $Q_{(0,\ Y)}$ represents the frictional heat flux along the interface between tool and chip.

Moreover, the two-dimensional domain (OABC) in both Figures 4(a) and (b) of the cutting tool is set as at orthogonal geometry, neglecting the nose radius. Then, OABC is discretised into, N_s sub-regions of triangular elements, which is not essentially of the similar dimensions. The locations of N_n nodes are specified and numbered beginning from the boundary nodes, $n = 1, 2, 3, 4, 5\ldots, N_b$, while the interior nodes similarly follow the pattern, as $n = N_{b+1}, N_{b+2}, N_{b+3}, \ldots, N_n$ so that a reliable solution from iteration operation for the temperature fields within the cutting tool (OABC) can be obtained.

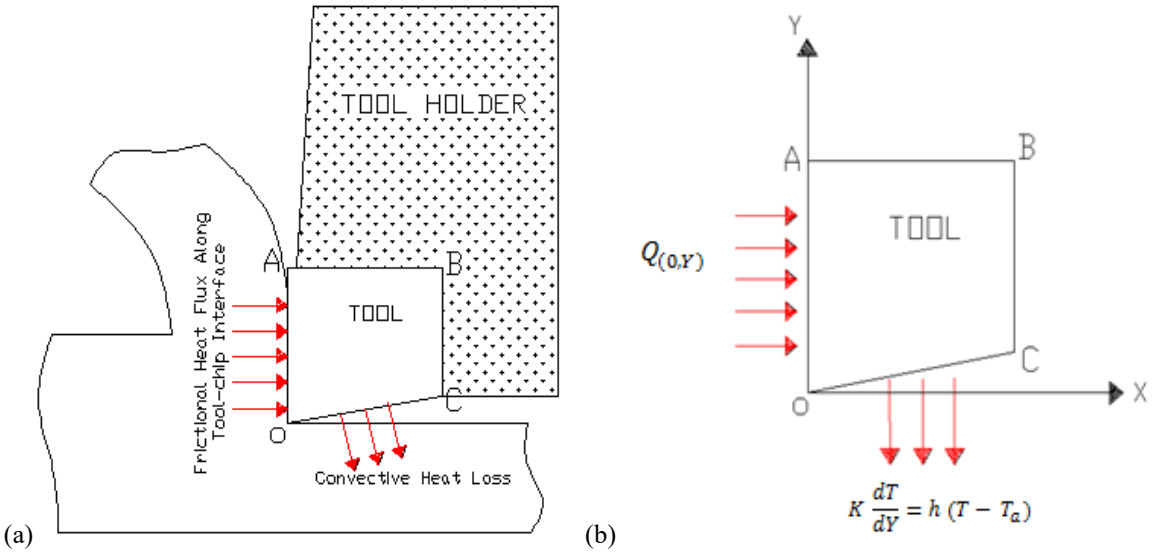

Figure 4 Schematic representation of heat flow and boundary conditions of the cutting tool.

3. Results and discussion

3.1 The average interfacial temperature, (T_{int}) between tool and chip

Both significant properties and cutting conditions of Al6061-T6, aluminum alloy used as a workpiece are stated in Tables 1(a) and (b), respectively. These quantities are used for the model validation.

Table 1(a) Mechanical and Thermal properties of Al6061-T6 (Strentowski and Moon, 1990).

Material Constants	Value	Unit
Density	2700	Kg/m^3
Thermal Conductivity	204	W/m.k
Specific Heat	896	J/kg.k
Yield Strength	276	MPa

Table 1(b) Cutting conditions of Al6061-T6, aluminum alloy (Strentowski and Moon, 1990).

Parameters	Value	Unit
Rake Angle	0, 30	Degrees Degrees
Feed Rate	0.13, 0.0635	mm/rev mm/rev
Speed	30 to 90, 30 to 150	m/min m/min

The model derived for the average interfacial temperature between tool and chip, T_{int} , as started in Equation (20) is simulated with MATLAB software and the corresponding results obtained are compared to experimental results from Strenkowski and Moon (1990), for validation. They experimentally measured the average interfacial temperature between tool and chip with thermocouples. Also, they machined Al6061-T6 tubes at different cutting situations. The cutting speeds were varied from 30 m/min to150 m/min for a rake angle of 30° and 30 m/min to 90 m/min for a rake angle of 0°. Furthermore, simulation was performed with the temperature model derived (Equation 20) in this study. The same machining conditions: workpiece conductivity of 204 W/(m·K), density of 2700 kg/m^3 and thermal capacity of 896 J/(kg°C) as well as Al6061-T6 aluminum alloy

workpiece material were used in order to compare and validate the model. Figures 5(a) and (b) evidently depicts that simulation results have a close similarity with the experimental measurement, as reported by Strenkowski and Moon (1990).

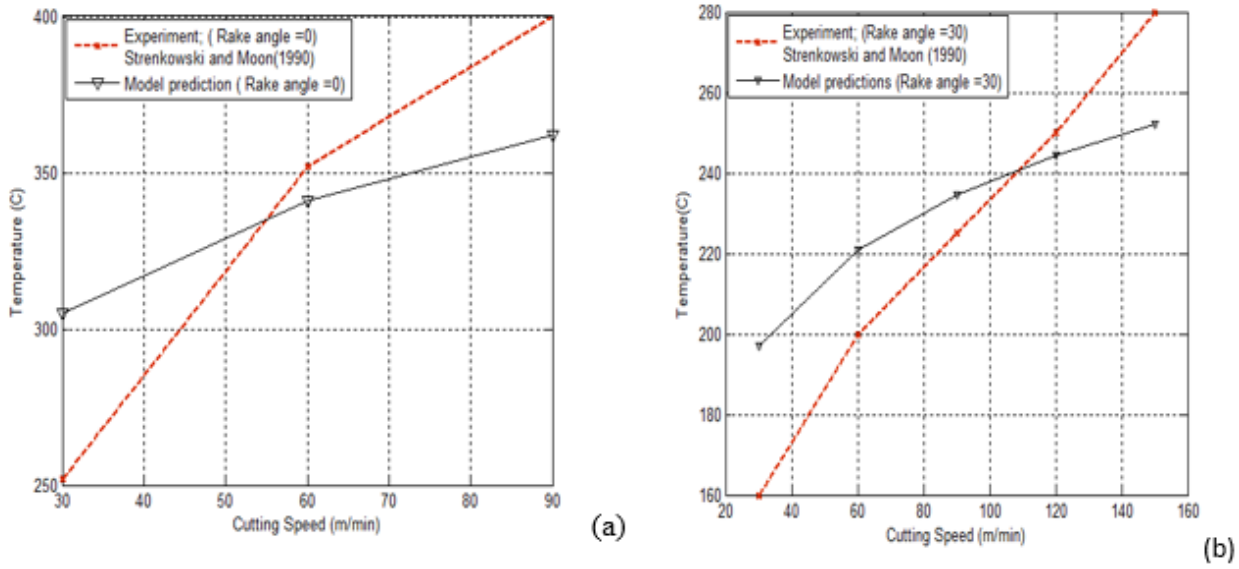

Figure 5 Comparison of model predictions and experimentally measured values, showing the effect of both rake angles of (a) 0º and (b) 30º and cutting speeds on the interfacial temperature between tool and chip.

The minimum temperature from the experiment by Strenkowski and Moon is approximately 250 ºC (for rake angle = 0º, at cutting speed = 30 m/min) while the model predicted 305 ºC under the same conditions. This discrepancy could be as a result of inaccuracy in determining the initial temperature of the primary shear region during simulation, since the heat produced in the primary shear area directly influences the interfacial temperature between tool and chip. But, as the cutting speed is further increased to a maximum cutting speed of 90 m/min, the temperature from the experiment was 400 ºC (at rake angle = 0º, at cutting speed = 90 m/min) while the model predicted 365 ºC under the same conditions. The underestimation by the model can be attributed to the inaccuracy in predicting the temperature of the primary shear area in the assumptions of the formulated model. A similar trend of the result was also recorded when rake angle of 30º and feed rate of 0.0635 mm/rev were used. Though the model result overestimates the average interfacial temperature at the inception of the cutting at speed of 30 m/min, it still approximately agrees with the experimental values as cutting speed rises.

In addition, in order to examine the influence of rake angle on the average temperature of the secondary shear zone, the cutting speed and depth of cut are set as 60 m/min and 2 mm, respectively, while the rake angle varies from -5º to 25º. It is observed from Figure 6 that as the rake angle increases, while the average interfacial temperature between the tool and chip decreases. This is due to the reduction in the friction force along the interface between the tool and chip as well as reduction in plastic deformation along the primary shear area. The reduction in the friction force is brought about by the decrease in the normal pressure and contact length

of the tool-chip interface along the rake face. Therefore, using large rake angles in machining operations minimises energy consumption by reducing frictional effect which occurs along the rake face.

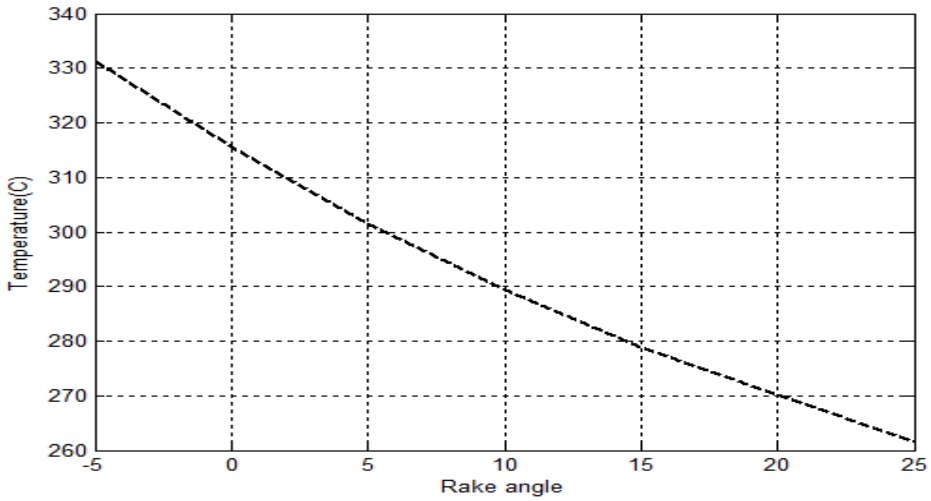

Figure 6 Influence of cutting tool rake angle on average interfacial temperature between the tool and chip.

3.2 Maximum tool temperature and tool temperature distribution

The effects of workpiece material yield strength, cutting speed as well as the feed rate on the maximum temperature of the cutting tool are depicted respectively in Figures 7, 8 and 9. The tool thermal conductivity and depth of cut used in the simulations are 40 W/m.K and 2 mm, respectively. It can be observed from the simulation results show that the maximum temperature, generates along the tool-chip interface occurs not at the tip of the cutting tool, but occurs at a particular region away from the tool tip. This implies that this region along the rake face of an orthogonal cutting tool is more susceptible to wear than the tool tip, due to excessive thermal loading.

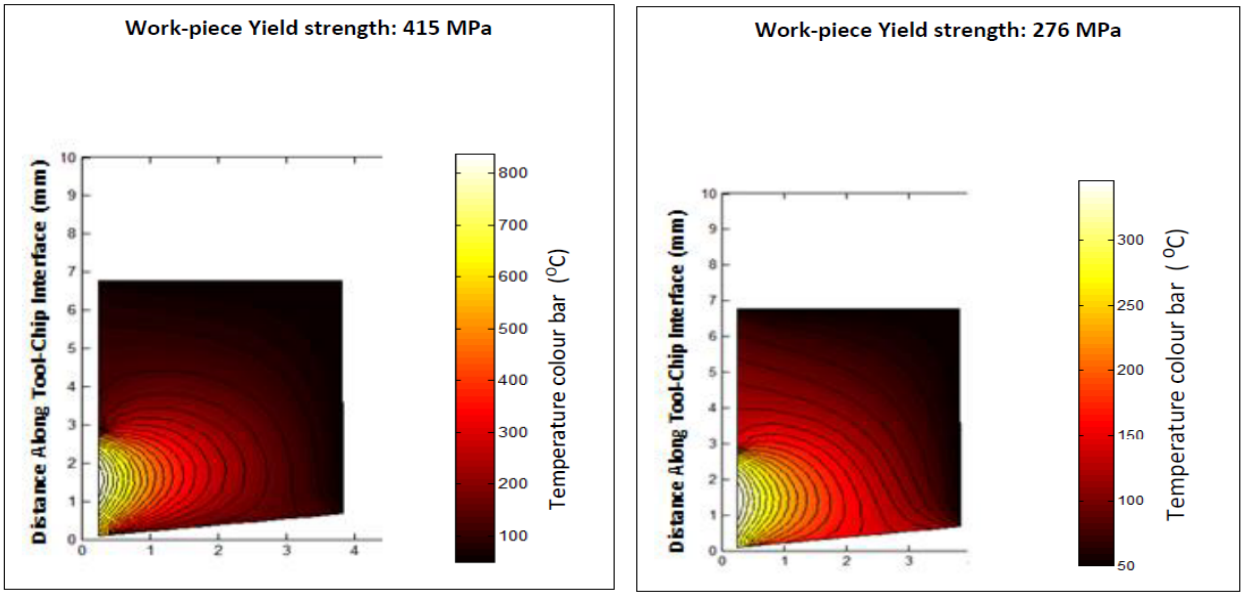

Figure 7 Influence of Al6061-T6 yield strength on the maximum temperature of the cutting tool.

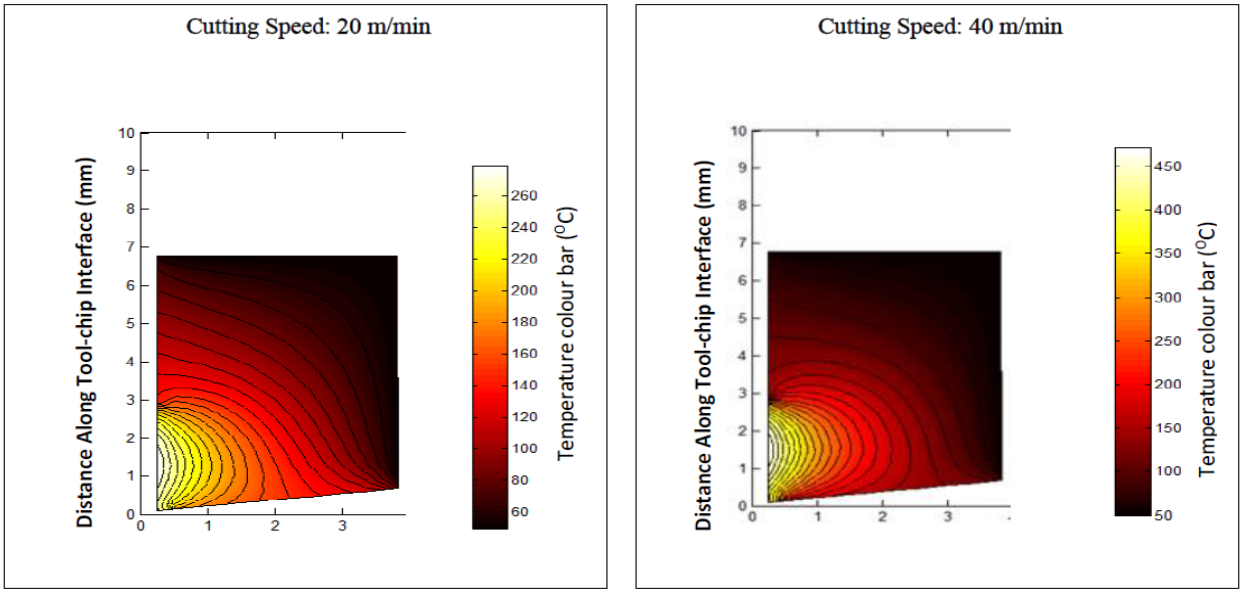

Figure 8 Influence of cutting speed on the maximum temperature of the cutting tool.

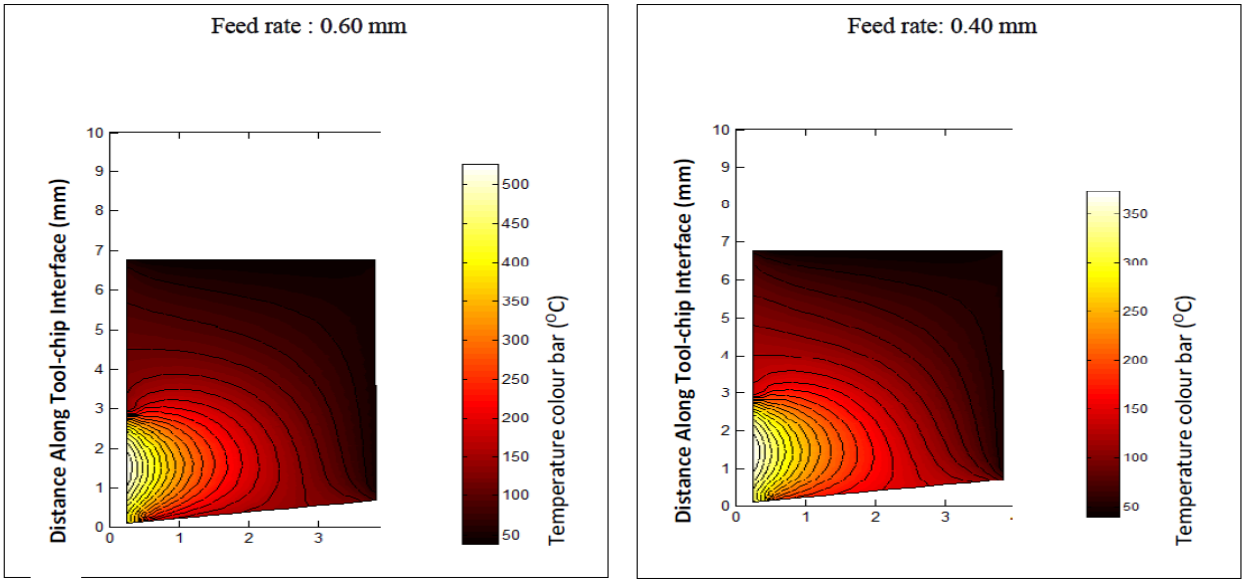

Figure 9 Influence of feed rate on the maximum temperature of the cutting tool.

From Figure 7, it is observed that an increase in the workpiece yield strength from 276 MPa (typical aluminum alloy) to 415 MPa (steel), while keeping other cutting parameters constant, increases the maximum temperature of the cutting tool along the interface between tool and chip. Also, Figure 8 shows that a rise in cutting speed, while keeping other cutting parameters (rake angle, feed, depth of cut, workpiece material and cutting tool) constant, produces a commensurate increase in the maximum cutting tool temperature along the interface between tool and chip. Similarly, Figure 9 depicts that the tool feed rate increased with the temperature at the interface between tool and chip. Summarily, before any cutting operation is implemented appropriate cutting conditions be selected and tested with this proposed mathematical model to ensure an optimised machining process, provided the cutting tool is not thermally loaded beyond limit.

4. Conclusions

This present study has reported an analytical model for friction and average interfacial temperature between tool and chip, derived by analysis of the mechanics of metal cutting in the orthogonal direction, as a function of the shear flow stress, rake angle, shear angle, cutting speed, depth of cut, as well as the length of the interface between tool and chip. The temperature fields within the cutting tool and along the tool-chip interface was established by using finite element method based on the analytical model derived with the MATLAB software. The simulation/model and experimental results were obtained and compared. The model was validated using experimental properties and cutting conditions of Al6061-T6 aluminum alloy (workpiece material). The model predictions showed a similar pattern to the experimental results. The minimum temperature obtained from the model was 220 ºC, at rake of 0º and cutting speed of 30 m/min. But, as the cutting speed was further increased to a maximum value of 90 m/min, the maximum temperature from the experiment and developed model were 410 ºC and 490 ºC respectively, at same rake angle of 0º. The minimum temperature from the predictive model was 140 ºC at rake angle of 30º and cutting speed of 30 m/min.

Based on the simulation results obtained, it was evident that the maximum temperature of the cutting tool (along the tool-chip interface) does not occur at the tool tip where pressure is maximum, but at a particular region away from the tool tip, which is consequently more susceptible to wear due to excessive thermal loading. Also, the effect of variation in workpiece material yield strength, cutting speed and feed rate on the maximum temperature of an orthogonal cutting tool showed that an increase in any of these independent variables significantly increased the temperature of the cutting tool. Therefore, before any cutting operation is implemented, appropriate cutting conditions should be selected and tested with this developed model to achieve an optimized cutting process, if the thermal load of the cutting tool is not exceeded.

Though, the simulation results underestimated the average interface temperature at the initial cutting speed of 30m/min, but significantly, the proposed mathematical models are in close agreement with the reported experimental results.

References

Abushawasi, Y., Xiao, X. and Astakhov, V.P. (2011) 'FEM simulation of metal cutting using a new approach to model chip formation', *International Journal of Advances in Machining and Forming Operations*, Vol. 3, No. 2, pp.71-92.

Alabi, A G.F., Ajiboye, T.K. and Olusegun, H.D. (2012) 'Investigation of cutting temperatures distribution in machine heat treated medium carbon steel on a lathe', *Journal of Engineering and Applied Sciences*, Vol. 7, No. 1, pp.113-122.

Altintas, Y. (2000) *Manufacturing Automation: Metal Cutting Mechanics, Machine Tool Vibrations, and CNC Design,* 1st ed., Cambridge University Press, UK.

Astakhov, V. P. (1999) *Metal Cutting Mechanics,* CRC Press, USA.

Astakhov, V. P. (2006) *Tribology of Metal Cutting,* 1st ed., Elsevier, London.

Astakhov, V.P. (2005) 'On the inadequacy of the single-shear plane model of chip formation', *International Journal of Mechanical Sciences*, Vol. 47, No. 11, pp.1649–1672.

Babu, B.G., Selladurai, V. and Shanmugam, R. (2008) 'Analytical modelling of cutting forces of end milling operation on aluminium silicon carbide particulate metal matrix composite material using response surface methodology', *ARPN Journal of Engineering and Applied Science*, Vol. 3, No. 2, pp.5-18.

Bayoumi, A.E., Yucesan, G. and Kendall, L. A. (1994) 'An analytical mechanistic cutting force model for milling operations: A theory and methodology', *Transactions of the ASME, Journal of Engineering for Industry,* Vol. 116, No. 3, pp.324-330..

Childs, T.H.C. (2006) 'Friction modeling in metal cutting'*, International Journal of Machine Tool and Manufacturing,* Vol. 260, No. 3, pp.310-318.

Dogra, M., Sharma, V.S. and Dureja, J. (2011) 'Effect of tool geometry variation on finish turning – A review', *Journal of Engineering Science and Technology Review*, Vol. 4, No. 1, pp.1-13.

Ezugwu, E.O. and Wang, Z. M. (1997) 'Titanium alloys and their machinability – A review', *Journal of Materials Processing Technology*, Vol. 68, No. 3, pp.262-274.

Gerez, J. M., Sanchez-Carrilero, M., Salguero, J., Batista, M. and Marcos, M. (2009) 'A SEM and EDS based study of the microstructural modifications of turning inserts in the dry machining of Ti6Al4V alloy'. *Proceedings of the AIP Conference*, Vol. 1181, pp. 567-574. https://aip.scitation.org/doi/abs/10.1063/1.3273676(Accessed 23 April, 2018).

Hartung, P. D., Kramer, B.M. and von Turkovich, B.F. (1982) 'Tool wear in titanium machining', *CIRP Annals*, Vol. 31, No. 1, pp.75-80.

Jam, J.E. and Fard, V.N. (2011) 'A novel method to determine tool-chip thermal contact conductance in machining', *International Journal of Engineering Science and Technology*, Vol. 3, No. 12, pp.8491-8501.

Kagnaya, T., Lazard, M., Lambert, L., Boher, C. and Cutard, T. (2011) 'Temperature evolution in a WC-6%Co cutting tool during turning machining: Experiment and finite element, *WSEAS Transactions on Heat and Mass Transfer*, Vol. 6, No. 3, pp.71-80.

Kegg, R.L. (1965) 'Cutting dynamics in machine tool chatter', *Transactions of the ASME, Journal of Engineering for Industry,* Vol. 87, No. 4, pp.464-470.

Kim, H.S. and Ehmann, K.F. (1993) 'A cutting force model for face milling operations', *International Journal of Machine Tools Manufacturing*, Vol. 13, No 5, pp.653-673.

Komvopoulos, K. and Erpenbeck, S.A. (1991) 'Finite element model of orthogonal metal cutting', *Transactions of the ASME, Journal of Engineering for Industry,* Vol.113, No. 3, pp.253-267.

Loschnner, P., Jaros, K. and Nieslony, P. (2016) 'Investigation of the effect of cutting speed on surface quality in abrasive water jet cutting of 316L stainless steel'. *Procedia Engineering*, vol. 149, pp. 276-282.

Mottaghizadeh, P. and Bagheri, M. (2012) '3D Modelling of temperature by finite element in machining with experimental authorisation', *World Academy of Science, Engineering and Technology*, Vol. 68, pp.1728-1734.

Moufki, A., Molinari, A. and Dudzinski, D. (1998) 'Modeling of orthogonal cutting with a temperature dependent friction law', *Journal of the Mechanics and. Physics of Solids,* Vol. 46, No. 10, pp.2103-2138.

Oxley, P.L.B. (1989) *Mechanics of Machining: An Analytical Approach to Assessing Machinability*, 1st ed., John Wiley & Sons, New York, USA.

Ozel, T. and Altan, T. (2000) 'Process simulation using finite element method-prediction of cutting forces, tool stresses and temperatures in high-speed flat end milling', *International Journal of Machine Tools and Manufacturing*, Vol. 40, No. 5, pp.713-738.

Pittalà, G.M. and Monno, M. (2011) 'A new approach to the prediction of temperature of the workpiece of face milling operations of Ti-6Al-4V', *Applied Thermal Engineering*, Vol. 31, No. 2-3, pp.173-180.

Salem, S.B., Bayrakrar, E., Boujelbene, M. and Katundi, D. (2012) 'Effect of cutting parameters on chip formation in orthogonal cutting', *Journal of Achievements in Material and Manufacturing Engineering*, Vol. 50, No. 1, pp.8-17.

Shih, A.J. (1995) 'Finite element simulation of orthogonal metal cutting', *Transactions of the ASME, Journal of Engineering for Industry,* Vol. 117, No. 1, pp.84-93.

Shih, A.J. and Yang, H.T.Y. (1993) 'Experimental and finite element predictions of residual stresses due to orthogonal metal cutting*', International Journal for Numerical Methods in Engineering,* Vol. 36, No.9, pp.1487- 1507.

Strenkowski, J.S. and Caroll, J.T. (19985) 'A finite element model of orthogonal cutting*', Transactions of the ASME, Journal of Engineering for Industry,* Vol. 107, No. 4, pp.349-354.

Strenkowski, J.S. and Mitchum, G.L. (1987) 'An improved finite element model of orthogonal cutting*'. Proceedings of the 15th North American Manufacturing Research conference.* May 27-29 May, 1987. Bethlehem, Pennsylvania, USA.

Strenkowski, J.S. and Moon, K.J. (1990) 'Finite element prediction of chip geometry and tool/workpiece temperature distributions in orthogonal metal cutting', *Transactions of ASME, Journal of Engineering for Industry,* Vol. 112, No. 4, pp.313-318.

Sultan, A.Z., Sharif, S. and Kumiawan, D. (2015) 'Effect of machining parameters on tool wear and hole quality of AISI 316L stainless steel in conventional drilling'. *Procedia Manufacturing*, vol. 2, pp. 202-207.

Tao, Z., Lovell, M.R. and Yang, J.C. (2004) 'Evaluation of interfacial friction in material removal processes: The role of workpiece properties and contact geometry', *Wear,* Vol. 256, No. 7-8, pp.664-670.

Ueda, K. and Manabe, K. (1992) 'Chip formation in micro cutting of an amorphous metal*', CIRP Annals,* Vol.41, No. 1, pp.129- 132.

Yen, Y.C., Söhner, J., Lilly, B. and Altan, T. (2004) 'Estimation of tool wear in orthogonal cutting using the finite element analysis', *Journal of Material Processing Technology*, Vol. 146, No. 1, pp.82-91.

Zhang, J, Liu, Z. and Du, J. (2015) 'Modelling and prediction of tool-chip interface temperature in hard machining of H13 steel with PVD coated tools', *International Journal of Machining and Machinability of Materials*, Vol. 17, No. 5, pp.381 – 396.

Biographies

Sunday J. Ojolo is an Associate Professor of Machinery Design and Manufacturing in Mechanical Engineering Department, University of Lagos, Nigeria. He attended Obafemi Awolowo University, where he studied Agricultural Engineering. He had his M.Sc. in Farm Power and Machinery and PhD in Biomass Energy (Wastes conversion and reuse) all from University of Ibadan, Nigeria. His area of research revolves round Biomass Gasification Technology, Renewable Energy, Machinery Development and Manufacturing Engineering. He is a member of American Society of Agricultural and Biological Engineers; American Society of Mechanical Engineers; and The Materials Society of America. He is a member of the Nigerian Institution for Standards (SON); he is a corporate member of Nigerian Society of Engineers and Fellow of the Nigerian Institution of Mechanical Engineers. He is a member of town planing community of Rehovot, Israel (JP). He was the Lead Academic on African Knowledge Partnership of British Council for synthesising biodiesel from Jatropha seeds. He was consultant for Waste from Energy Incorporation, California (USA) to charatarize Olososun Waste for energy generation. He is currently the Director of Information and Communication Technology Resource Centre, Bells University of Technology, Ota. He has featured in Young Inventors of Nigeria Television Authority (NTA).

Sikiru Ismail is Lecturer I in Mechanical Engineering Department, University of Lagos. He had his B.Sc. in Mechanical Engineering from Federal University of Technology, Akure, Nigeria. He had his M.Sc. in Mechanical Engineering from University of Lagos, Nigeria and holds a PhD in Mechanical Design from Postmouth University, UK. His area of specialisation is in Machinery Design and Manufacting Engineering.

Kelechi Ogbuanu is a PhD candidate in Mechanical Engineering at University of Delaware, USA. He had his B.Sc. and M.Sc. in Mechanical Engineering from University of Lagos, Nigeria.